

Eye-Box Measurement for Augmented-Reality Waveguides with Pupil Expansion

Xin Li*, Chengzhe Chai*, Yining Li*, Lei Zhao*

*Advanced Display and Sensing Research Center, *YONGJIANG Laboratory, Ningbo, Zhejiang, China

Abstract

The eye box is an important index in near-eye display which describes the three-dimensional stereo space in which the near-eye display device can clearly and completely see the virtual image, and the size of the eye box determines the range of positions in which the near-eye display device can accommodate the movement of the eye for users with different pupil distances. Conventional methods based on luminance or MTF scanning of the near-eye-display are a time-consuming process, and the eye box luminance uniformity of the extended waveguide in augmented reality will make it more difficult to unify the selection of the reference and the threshold luminance. Therefore, this paper proposes an eye box measurement for augmented reality devices with pupil extended, which is based on the analysis of the light distribution from the boundary view outside the eye box, by analyzing the parameters of spot separation, combining the field of view and then calculating the size of the eye box at a particular eye relief, the method can also be used to determine the three-dimensional stereo size of the eye box of a near-eye display device. Therefore, the method can also be used to determine the 3D stereo dimensions of the eye box. The method is efficient and fast as it only requires the light spot distribution map of the boundary view outside the eye box region to analyze the 3D dimensions of the eye box.

Author Keywords

Augmented reality; Eye box; Pupil-extended.

1. Introduction

With the booming development of microdisplay technology and high-speed digital processors, augmented reality (AR) technology has gradually landed on the ground, and related terminal products have begun to emerge and become more and more popular. By superimposing virtual content on the real world, AR enhances our perception and immersion in the environment. Combined with the rapidly iterating AI technology of recent years, AR+AI offers considerable possibilities for the development of meta-universes and digital twins^{1,2}.

The eye box describes a three-dimensional stereoscopic space, also called Qualified Viewing Space (QVS), in which the user's eyes can see the virtual image clearly and completely in this three-dimensional space, so the size of the eye box is an important performance indicator for near eye devices, which determines the range of eye positions that can be accommodated by the near-eye display device to cover the immersive experience of virtual content for user groups with different pupil distances.

Conventional measurement of eye box requires first determining the location of the eye point, and then scanning the luminance or Modulation Transfer Function (MTF) in the plane perpendicular to the optic axis with an AR/VR lens, and when the luminance or MTF drops to a certain threshold, it is considered to be the eye box boundary. Repeated scanning by changing the distance in the direction of the optic axis can get the 3D size of the eye box, and the process of this method is very time-consuming and inefficient. In addition, the location of the eye point of the AR device is more

difficult to confirm, and the uniformity of the luminance of the eye box very much affects the selection of the threshold value³. Therefore, new methods need to be proposed to characterize the eye box for pupil-extended optical waveguides.

Hong^{4,5} proposed a method which places a diffuse reflective screen at the user's eye position, the light forms a luminance distribution image on the diffuse reflective screen, and the overlapping part of the luminance distribution is the eye box area, the luminance distribution on the diffuse reflective screen is captured by a camera and analysed to obtain the eye box size. However, for devices with poor luminance uniformity of the eye box, this method is very difficult to identify the boundary of the overlapping part, and if we want to obtain the 3D spatial dimensions, we also need to obtain the luminance distribution images of multiple positions in the z-direction. Varshneya⁶ proposed a Draper method that maps the boundaries of display performance limiting aperture by capturing two virtual images at short pupil distance and long pupil distance positions, which in turn computes the 3D eye box.

According to the optical characteristics of the extended optical waveguide, the method proposed in this paper focuses on the spot distribution of the boundary view outside the eye box region, obtains the spot distribution image directly through the 2D sensor, analyses its separation parameter, combines with the field of view (FOV) of the device to be tested, and substitutes it with different eye reliefs to get the 3D eye box. Then, we compare the method with other eye box measurement methods to prove its feasibility, and apply the method to both diffraction and array pupil extended waveguides to prove its universality.

2. Theory

Figure 1 illustrates the principle of optical waveguide pupil expansion, taking the reflection diffraction waveguide as an example, when the beam passes through the coupling into the original, it enters the waveguide propagation, and when the beam propagates to the coupling out grating, a part of the light energy is diffracted out of the waveguide every time, while the remaining light energy continues to be transmitted in the waveguide until it again interacts with the coupling grating to diffractively coupling out of the waveguide so that the light beam is continuously replicated, and the expansion is finally achieved.

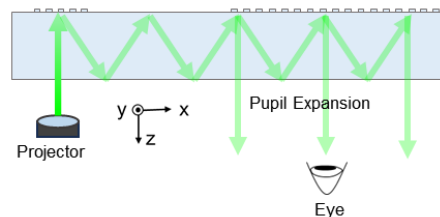


Figure 1. Pupil expansion schematic.

Fig. 2(a) illustrates the schematic cross-section (x-y plane) of a pupil extended optical waveguide, the green arrow represents the light from the upper boundary of the virtual image, in the process

of extended pupil downward propagation, while replicating the coupling out to the right, and then propagated through the free space for a distance, the spot distribution will be biased downward, such as the green dashed line in Fig. 2(b) in the region framed. Similarly, the spot distribution of the light from the upper boundary of the virtual image is biased upward, as in the region framed by the red dashed line in Fig. 2(b). The spot distribution from the left and right boundary light of the virtual image is coupled out to the right and left, respectively, as shown in the yellow and blue dotted lines in Fig. 2(b). Which when the eye in the overlap region can see full image, so the overlap region that is the eye box, the eye box boundary is mainly determined by the virtual image of the upper and lower, left and right boundaries of the spot.

However, due to the poor uniformity of the luminance of the eye box, the overlap region boundary is often difficult to determine, as shown in Figure 3.

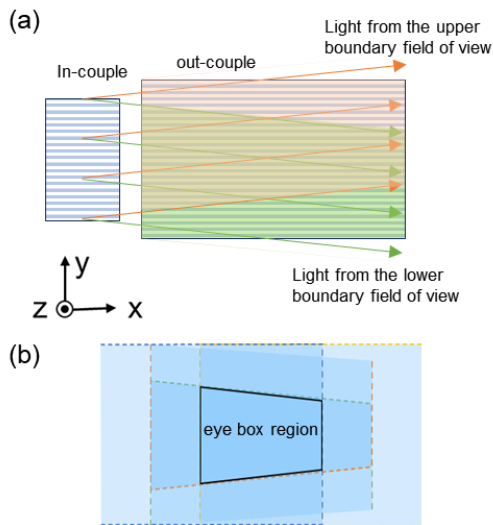


Figure 2. The eye box with extended waveguide. (a) Schematic illustration of the transmission of light from the upper and lower boundaries through the extended pupil. (b) In eye relief, the eye box, i.e., (black closed line) left (yellow dashed line) right (blue dashed line) border field of view of the light spot overlap area.



Figure 3. The luminance distribution of the eye box. The overlapping part, i.e. the eye box boundary, is difficult to distinguish.

Figure 4 shows the schematic calculation of the method proposed in this paper, placing a 2D Sensor outside the eye box region in the direction of the optic axis, we will get the spot distribution of the two viewing angles, there is no luminance distribution near the optic axis, and the boundaries are easy to distinguish.

Therefore, the luminance distribution parameter of the spot in the boundary view outside the eye box in the direction of the visual axis can be analysed to calculate the size of the eye box under a certain eye relief, and the following equations give the specific calculation process of the size of the eye box:

$$\begin{aligned} Y_x &= \tan \theta_V(L - L_i) - p * y_x \\ X_y &= \tan \theta_H(L - L_i) - p * x_y \end{aligned} \quad (1)$$

Where p is the pixel pitch of the CMOS, V is the longitudinal half-field-of-view angle, H is the horizontal half-field-of-view angle, Y_x is the vertical coordinates of the upper and lower boundaries of the eye box at eye relief, X_y is the horizontal coordinates of the left and right boundaries of the eye box, L_i represents the different eye relief distances, and L is the distance between the CMOS and the optical waveguide.

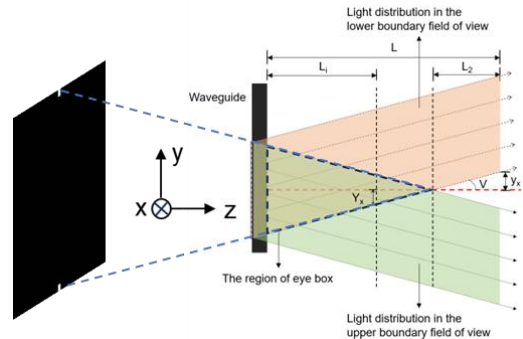


Figure 4. Schematic of the spot distribution, with the light from the upper and lower image's boundary.

3. Experiment

The experimental setup is shown in Fig. 5, which contains the AR device to be tested and a CMOS, the CMOS is placed outside the eye box region in the visual axis direction, and the boundary FOV image is fed to the device to be tested, and the light from the input image is coupled out by waveguide conduction, presenting a separated spot distribution on the CMOS, a JCOPTIX color CMOS camera (AIC-2000C-USB) was used for the CMOS, and the resolution is 5488×3672 pixels. 2000C-USB with a resolution of 5488×3672 pixels and a pixel pitch of $2.4 \mu\text{m}$.

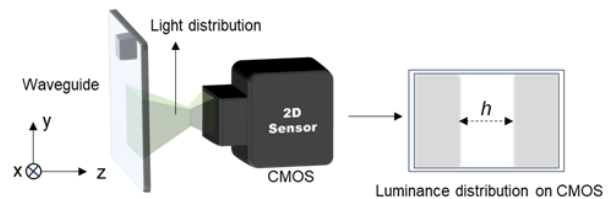


Figure 5. Schematic of the experimental setup used for measuring the eye box in augmented reality waveguides.

Firstly, input the specific pattern to the device to be tested and playback the display, adjust the relative position of CMOS and the device to be tested to ensure that the CMOS can receive the output light signal, adjust the distance between CMOS and the optical waveguide until the spot separation can be seen on the CMOS, output the distribution map, and record the distance between CMOS and the optical waveguide, L . Then, carry out pre-processing on the distribution map such as histogram equalisation, morphology operation, sharpening Then the

distribution map is preprocessed with histogram equalisation, morphological operation, sharpening and Gaussian blurring, and the image is enhanced in the excessive region, the image and the retrograde threshold segmentation are realised to extract the contour boundary, and based on the parameter of statistical separation of the contour boundary, the separation distance y_x is calculated, and finally, combining with the horizontal and longitudinal field-of-view angles of the device, H and V, the size of the eye box at the distance L_i is calculated according to Equation (1).

4. Results and Discussion

In order to verify the feasibility of the method, the array optical waveguide is selected as the device to be tested, DUT1, which has a FOV of $21^\circ \times 13^\circ$. The FOV luminance of DUT1 is captured with a large FOV AR/VR camera calibrated for pixel angular resolution, as shown in Fig. 6(a), from which the horizontal and vertical FOV of the virtual image can be analysed. The previous analysis shows that the overlapping part of the luminance distribution formed after the light from the boundary of the virtual image is coupled out from the waveguide is the eye box region, so the experiment adopts the image shown in Fig. 6(b) to input into the DUT1, and then adopts the device shown in Fig. 4 to obtain the luminance distribution in the direction of the optic axis outside of the eye box, as shown in Fig. 6(c). Since only the boundary pixels of the virtual image are bright, there is no light distribution in the direction of the visual axis outside the eye box region, and a luminance distribution map with a dark center as shown in Fig. 6(c) will be obtained. Image preprocessing is performed to extract the contour boundaries to get what is shown in Fig. 6(d), which is processed to get the parameters y_x and x_y of the contour. Finally, the 3D eye box is calculated according to Equation 1, as shown in Fig. 7.

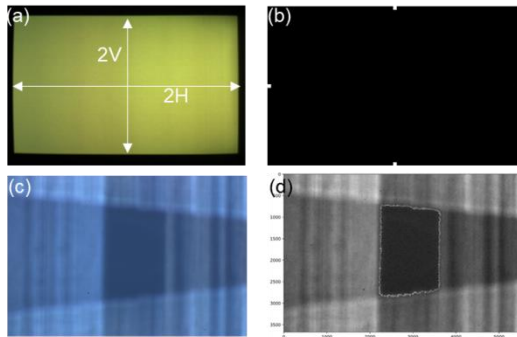


Figure 6. (a) Luminance distribution of the field of view of DUT1. (b) Schematic of the input image of DUT1. (c) Luminance distribution obtained by CMOS outside the eye box region in the view-axis direction. (d) Contour extraction map after pre-processing of Fig. (c).

To demonstrate the validity of the method, this paper compares the results with the Scanning and Draper methods at eye relief = 15 mm. The Scanning method is the eye box measurement method for near-eye display devices in the IEC standard, this method needs to determine the eye point position first, and then scan the luminance distribution of the boundary view angle in the x-y plane, using the luminance of the 0-view angle of the eye point position as the benchmark, and when the luminance of each boundary view angle decreases to a certain threshold of the benchmark luminance, it is regarded as the boundary of the eye box. For this test, a Gamma scientific E101 device was used, and the eye point position was determined by the center of the eye box

at view 0° , with a threshold of 50%, and the eye box was scanned both horizontally and vertically.

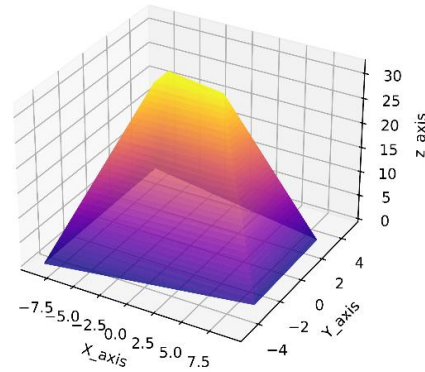


Figure 7. The 3-dimensional eye box distribution of DUT1.

The Draper method uses a FOV AR/VR camera (Gamma Scientific W200) calibrated with pixel angular resolution to obtain the luminance distributions of the virtual image at short and long pupil distances, and then calculates the eye box, which is 60 mm at long pupil distance for this Draper test. The eye boxes measured by the three methods at eye relief = 15 mm are shown in Fig. 8, and the horizontal and vertical dimensions are summarised for the three methods. The horizontal and vertical dimensions of the three methods are summarised in Table 1.

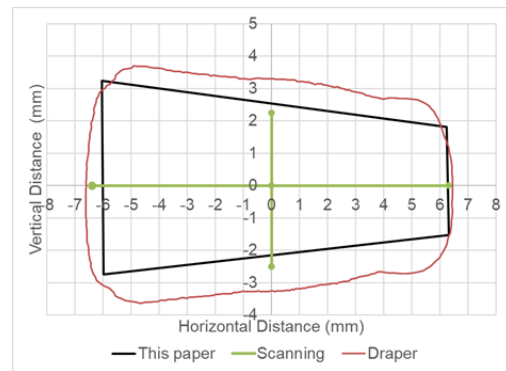


Figure 8. The eye box measured by the three methods when eye relief was 15 mm.

The results in Fig. 8 show that there is a difference between the eye box size measured by the method in this paper and the other two methods. The results of the scanning method are slightly larger, which is mainly due to the differences in the measuring principle and the equipment used, specifically due to two reasons: firstly, there is a difference in the reference viewing angle, scanning is mainly based on the luminance change of the boundary of the 2° FOV, while the pixels of this paper's method account for about 0.3° FOV; Secondly, because the scanning measurement uses a 4 mm entry-pupil diameter AR/VR lens, it can capture the full image even if it is slightly beyond the eye box.

Table 1. Comparison of measured data

Eye box	Scanning	Draper	This paper
Eye box_X (mm)	12.7	12.9	11.9
Eye box_Y (mm)	4.8	6.8	4.5

Fig. 9 shows the horizontal and vertical dimensions of the present method and Draper's method at different eye relief, and the trend of reduction with increasing distance is basically the same for both methods.

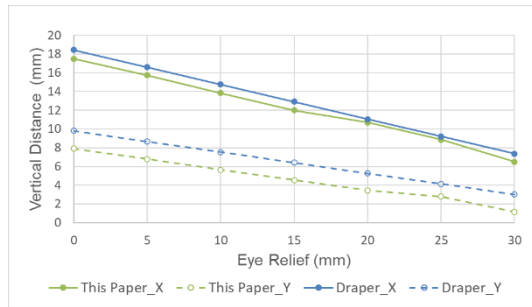


Figure 9. The trend of eye box with eye relief.

The eye box measured by the Draper method is larger in size and has roughly the same shape, but it is more rounded. It is assumed that because the Draper method uses a full image to measure, the eye box is the effect of the superposition of the extended light fields of the multiple viewpoints at the boundaries, so it is larger in size and more rounded in shape, and it needs to be further verified by designing experiments.

In order to prove the universality of the methods, this paper is based on three methods with the addition of a diffractive waveguide for testing DUT2. DUT2 is a two-dimensional pupil extended diffractive optical waveguide with a FOV of $22.5^\circ \times 17^\circ$. The test results are shown in Fig. 10, and the differences in eye box measured by the three methods are small, which can be used to characterise the three-dimensional distribution of eye box in AR.

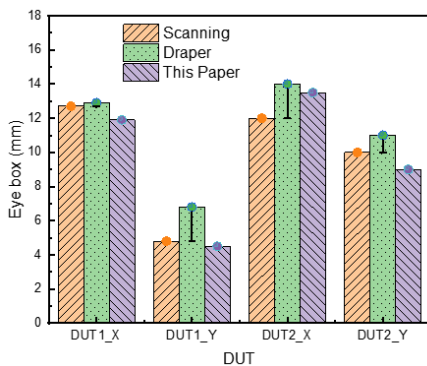


Figure 10. The eye box for two types of DUTs was measured using three methods.

5. Discussion and Conclusion

In this paper, a 3D eye box measurement method is proposed for the extended AR optical waveguide, which uses CMOS to directly obtain the spot distribution of the image boundary in the direction of the vertical visual axis outside the eye box, and then

analyze the parameters of the spot luminance distribution, combine the FOV of the device and the distance between the sensor and the waveguide to get the size of the eye box, and then substitute it into the eye box by fitting the eye box to the different eye relief. The three-dimensional distribution of the eye box can be fitted by substituting different eye relief. This method does not need to confirm the eye point, no need to scan point by point, only a brightness distribution outside the eye box area, and the FOV distribution of the device to be tested can be calculated to get the three-dimensional size of the eye box, which greatly improves the efficiency of the measurement, and the brightness distribution outside the eye box is more conducive to image processing.

6. Acknowledgements

This research was supported by Key R&D Program of Zhejiang No.2024SSYS0047.

7. References

- Xiong J, Hsiang EL, He Z, Zhan T, Wu ST. Augmented reality and virtual reality displays: emerging technologies and future perspectives. *Light Sci Appl* [Internet]. 2021 Oct 25 [cited 2023 Nov 28];10(1):216. Available from: <https://www.nature.com/articles/s41377-021-00658-8>
- Ding Y, Gu Y, Yang Q, Yang Z, Huang Y, Weng Y, et al. Breaking the in-coupling efficiency limit in waveguide-based AR displays with polarization volume gratings. *Light Sci Appl* [Internet]. 2024 Aug 12 [cited 2024 Aug 19];13(1):185. Available from: <https://www.nature.com/articles/s41377-024-01537-8>
- Ni D, Cheng D, Liu Y, Wang X, Yao C, Yang T, et al. Uniformity improvement of two-dimensional surface relief grating waveguide display using particle swarm optimization. *Opt Express* [Internet]. 2022 Jul 4 [cited 2024 Feb 1];30(14):24523. Available from: <https://opg.optica.org/abstract.cfm?URI=oe-30-14-24523>
- Hong H. Novel method for the fast measurement of the three-dimensional range of the eyebox of a VR device. *J Soc Inf Display* [Internet]. 2020 Sep [cited 2023 Aug 2];28(9):752–8. Available from: <https://onlinelibrary.wiley.com/doi/10.1002/jsid.871>
- Hong H. Fast Measurement of Eyebox and Field of View (FOV) of Virtual and Augmented Reality Devices Using the Ray Trajectories Extending from Positions on Virtual Image. *Current Optics and Photonics* [Internet]. 2020 Aug 25 [cited 2023 Oct 25];4(4):336–44. Available from: <https://doi.org/10.3807/COPP.2020.4.4.336>
- Varshneya R, Draper RS, Penczek J, Pixton BM, Nicholas TF, Boynton PA. 50-4: Standardizing Fundamental Criteria for Near Eye Display Optical Measurements: Determining the Eye-box. *SID Symposium Digest of Technical Papers* [Internet]. 2020 Aug [cited 2023 Jul 31];51(1):742–5. Available from: <https://onlinelibrary.wiley.com/doi/10.1002/sdtp.13975>